Hindawi
Advances in Civil Engineering
Volume 2018, Article ID 2915924, 8 pages
https://doi.org/10.1155/2018/2915924

Research Article

Quantification of the Transparency of the Transparent Soil in Geotechnical Modeling

Li-Da Yi,[1,2] Hua-Bin Lv,[1] Tian Ye,[1] and Yi-Ping Zhang[1]

[1]*College of Civil Engineering and Architecture, Zhejiang University, 866 Yuhangtang Road, Hangzhou, Zhejiang, China*
[2]*Power China Huadong Engineering Co., Ltd, 201 Gaojiao Road, Hangzhou, Zhejiang, China*

Correspondence should be addressed to Yi-Ping Zhang; zhangyiping@zju.edu.cn

Received 11 April 2018; Revised 2 July 2018; Accepted 15 July 2018; Published 9 September 2018

Academic Editor: Yonggui Chen

An indispensable process of geotechnical modeling with transparent soils involves capturing and analyzing images, in which favorable transparency is required for optical measurements. This paper proposes an objective framework for quantification of transparency in transparent soil based on its transmittance. Specifically, transparent soil with fused quartz serves as the soil sample for the detection of transmittance, and transmittance's impact on imaging quality in geotechnical modeling with transparent soil is investigated through an evaluation function of image clarity. According to the results of research about transparent soil with fused quartz, viewing depth and refractive index matching are the dominant factors that affect variations in transmittance of transparent soil, and the variations of transmittance are subjected to exponential decay regarding viewing depth or refractive index matching based on the theoretical modeling's function of curve fitting. Moreover, experimental results indicate that imaging quality of geotechnical modeling with transparent soil is enhanced with increasing transmittance, and imaging quality shows a remarkable improvement when transmittance is greater than 90%.

1. Introduction

For geotechnical testing, transparent soil is perceived as a model to visualize the internal geotechnical properties, such as deformation, strain, and flow [1]. It is a porous medium, which consists of a transparent surrogate representing natural soil and fluids with a matched refractive index. Transparent soil provides approaches for geotechnical modeling of soil-structure interactions and multiphase flow in soils [2]. Pioneering researchers of transparent soil introduced precipitated silica to investigate non-Newtonian fluid flow [3] and conducted further research on the geotechnical properties of low-plasticity clay [4, 5]. Over time, other families of transparent soils have been developed for geotechnical testing, including silica gel [6], hydrogel [7], fused quartz [8], and laponite [9]. In addition to investigation of soil-structure interaction mechanisms and hydraulic behavior, notable work has recently extended geotechnical applications of transparent soils to centrifuge tests [10], soil mechanics lessons in elementary schools [11], and research involving geo-environmental models [12].

In addition to the ability of transparent soil to model natural soil, visualization of the transparent soil is of equal importance to application in geotechnical testing. An indispensable process of modeling with transparent soil involves capturing and analyzing images. By capturing continuous images in noninvasive measurements, including digital image correlation (DIC), transparent soil techniques rival apparatuses such as X-rays, computerized tomography (CT), and magnetic resonance imaging (MRI) [13]. DIC serves as a methodology of image analysis for measurement of kinematics within transparent soils [14], in which transparency is required.

To determine a favorable level of transparency for optical measurements, the transparency of transparent soil has been evaluated in recent studies. For example, grid lines were observed through some viewing depth of transparent soil to rank different levels of transparency for possible analysis [15]; an adapted Snellen chart was utilized in an "eye test"

calibration for viewing decreasing font-sized letters through transparent soils to estimate the transparency that is available for visualization [16]. However, the conventional methodology of the above assessments is subjective and nonquantitative and infers variable levels of acceptable transparency for visualization of transparent soils. Thus, a comprehensive, objective, quantitative, and robust framework of transparency assessment awaits development. Recently, the modulation transfer function (MTF) has been proposed for quantitative assessment and comparison of transparency [17].

However, MTF is determined according to the fidelity of transferred details from object to image, which involves an overall imaging capability of the whole optical system, which is characterized by not only transparency of transparent soil but also the photographic apparatus. Hence, in order to provide observations of how transparency affects the accuracy of imaging and measurement in transparent soil, the purpose of this research is to quantitatively evaluate the transparency of transparent soil itself. If such a framework of evaluation is developed for the optical characteristics of transparent soil, it shall provide guidance for modeling experiments of transparent soil to reduce limitations on geometry and refractive index matching.

Specifically, in this paper, an objective framework for quantification of transparency based on transmittance is established by combining geotechnical engineering and optics. First, the calculation method of transmittance and the experimental setup for detecting transmittance is proposed so that transmittance data of transparent soil are acquired. Second, it is suggested that variations of transmittance are subjected to exponential decay, which is well explained by the principle of the Christiansen effect. And such observation of transmittance shall provide approaches to improving transparency quality of transparent soil. Third, for experiments of detecting transmittance for different transparent soil samples, experimental results and digital images demonstrate the relationship between transmittance and imaging quality of visualization in transparent soil. The relationship between transmittance and imaging clarity is investigated using an evaluation function of the digital image.

2. Objective Framework for Quantification of Transparency in Transparent Soil Based on Transmittance

2.1. Transmittance. Transmittance defines the property that a substance permits transmitted light to pass through, while incident light is partially absorbed or scattered. It is the mathematical description of transparency. The theory of radiometry indicates that transmittance T is the luminous flux ratio of transmitted light φ_t to incident light φ_i [18], which is expressed as

$$T = \frac{\varphi_t}{\varphi_i}. \tag{1}$$

The luminous flux refers to the power of electromagnetic radiation, which is modified due to varied sensitivity of the human eye to different wavelengths of light. It is calculated by a luminosity function regarding the issue. In the luminosity function, luminous efficacy is the weighting coefficient that represents the ratio of the luminous flux to the radiant flux. For a certain wavelength of light, the luminous flux φ is expressed as

$$\varphi = K_\lambda P, \tag{2}$$

where K_λ refers to the weighting coefficient at wavelength λ and P refers to the radiant flux. Based on (1) and (2), transmittance is denoted by the following equation:

$$T = \frac{P_t}{P_i}, \tag{3}$$

where P_t and P_i refer to the radiant flux of transmitted and incident light, respectively. Hence, the calculation method is capable of acquiring transmittance using optical measurements of a laser power meter in the experimental setup.

2.2. Measurement Method for Transmittance

2.2.1. Material. In the experimental setup, fused quartz, which is common in manufacturing, is applied as the solid particle of transparent soil. During the manufacturing process, fused quartz is highly purified by melting at approximately 2000°C and is formed by crystalline silica with a purity level of 99.9% to 99.95% [1]. Specifically, for the selected fused quartz in this research, it is shown in Figure 1 that the particle size ranges from 2.00 to 2.80 mm. At each wavelength of visible light, transmittance of fused quartz is well beyond 90%. The refractive index of fused quartz is reported as 1.4585 [19].

Fused quartz aggregate is matched with a blend of two oils, namely, 15# PURITY FG WO white mineral oil produced by Petro-Canada and EI solvent oil produced by TEACSOL. Both oils are transparent as well as colorless, with the physical properties that are listed in Table 1.

As listed in Table 1, higher flashing points of flammability indicate that the oils are safe to use under normal laboratory conditions at room temperature. Since the density of mineral oil is similar to that of EI oil, mixtures of such two oils are well blended. The refractive index of well-blended oils changes with the specific blending ratio to achieve different levels of refractive index matching. The refractive index is then measured by implementation of a 2WAJ refractometer with a precision of 0.0002. However, there is considerable variation in the refractive index of matching liquids at different temperatures [20]. To investigate the variation of the refractive index due to changing temperature, configuration of the DK-S18 water bath and circulating pump is connected to the refractometer for maintaining a constant temperature of the matching liquid [8, 21]. On the basis of the Arago-Biot function [22], the relationship between the resulting refractive index and blending ratio is expressed by the following equation:

Figure 1: Selected particle of fused quartz.

Table 1: Physical properties of the pore fluid.

Matching liquid	Flashing point (°C)	Density (kg/L)	Refractive index (at 20°C)
15# white mineral oil	180	0.847	1.4662
EI solvent oil	83	0.796	1.4380

$$n_{12} = \lambda\left[\theta n_1 + (1-\theta)n_2\right] + g, \tag{4}$$

where n_{12}, n_1, and n_2 refer to the refractive index of blended liquids, the first matching liquid, and the second matching liquid, respectively; θ refers to the volume fraction of the first matching liquid; and λ or g refers to the coefficient determined by temperature. Specifically,n_{12} represents the refractive index of blended oils and θ represents the volume fraction of the 15# white mineral oil. For the following experiment, the room temperature is strictly maintained as 20°C using an air conditioner, whereas λ and g are experimentally determined as 1.0159 and −0.0232 based on the calculation of the blending ratio.

2.2.2. Experimental Apparatus. For optical measurements, the layout of the experimental setup is shown in Figure 2(a), which involves a laser transmitter that emits 532 nm laser light, a test chamber, a detector of light power, and a laser power meter for detecting transmitter light power. As also shown in Figures 2(b) and 2(c), the test chambers provide desirable ranges of viewing depth, and a cuvette or acrylic glass box serves as the test chamber, with identical wall thickness on each side. When a light beam from a laser transmitter passes through transparent soil in the test chamber, the radiant flux of transmitted light P_t is measured. Then, the radiant flux of incident light P_i is measured without transparent soil in the test chamber. P_t and P_i are measured from multiple incident positions of light at one side of the test chamber. The side of the test chamber for incident light was switched over for each measurement of the transparent soil sample. Specifically, the incident positions of light are located roughly equidistant. In this way, 16 pairs of P_t and P_i are acquired for each measurement. On the basis of the 16 pairs of experimental results, the average results of transmittance are calculated. Moreover, the confidence interval of the average transmittance is also denoted as the error bar in the figures.

2.3. Variation in Transmittance

2.3.1. Principle of the Christiansen Effect. To investigate the variation in transmittance of transparent soil and to analyze the qualitative relationship between the factors (that affect the variation in transmittance) and the transmittance, the principle of Christiansen effect is proposed for the curve fitting of experimental results of transmittance of transparent soil. Preparation of transparent soil should ensure that the transparent substance is immersed in the refractive index matching liquid, which is also involved in the process of producing transparent media in the experiment of the Christiansen effect [23]. Numerous solid-liquid interfaces exist within such transparent media. For incident light with a specific wavelength on the solid-liquid interface, the principle of the Christiansen effect indicates that when dispersion curves of solid and liquid coincide at specific wavelength, incident light in Christiansen experiment is mostly transmitted [24]. Either the optical interference or the scattering results in attenuation of transmitted light in the Christiansen effect. The theory of the Christiansen experiment is concluded from optical interference [24], and it states that the transmittance of transparent media undergoes exponential decay. Particularly within transparent soil, incident light is scattered and refracted consecutively on multiple solid-liquid interfaces while transmitted light is attenuated. Assuming that inhomogeneity of random packing in solid particles has a Gaussian distribution in the refractive index [25], a modified equation of the Raman Varshneya [26] method is derived as follows:

$$T = \exp\left\{-\frac{k_1^2\pi^2\left[\ n_s - n_l\right)^2 + k_2\right]d}{\lambda_m^2}\right\}, \tag{5}$$

where n_s and n_l refer to the refractive index of the solid and liquid, respectively; k_1 refers to the coefficient that is modified by the size, shape, and distribution of the solid particle; k_2 refers to the coefficient that is modified by the shape and volume fraction of the solid particle; d refers to the transmitted thickness or viewing depth; and λ_m refers to the matching wavelength at which the solid and liquid refractive indexes are matched.

The principle of the Christiansen effect is the theoretical basis of this research that explains the factors that affect transmittance in optical measurements of transparent soil. With a consistent combination of grain size gradation and compactness within transparent soil, the subsequent impacts of size, shape, and distribution of solid particles are neglected in the following analysis. Besides, the modified equation of the Raman Varshneya method shall be utilized to provide observations into the function of curve fitting of the factors and to provide explanations on statistical parameter's physical meaning. Therefore, coefficients k_1 and k_2 remain constant for the same transparent soil sample. For the experimental setup in this study, the wavelength of transmitted light is maintained constant as 532 nm. Therefore, the viewing depth d and the refractive index matching $(n_s - n_l)$ are the main factors that affect transmittance, and they are analyzed in following verification experiments. For transparent soil with

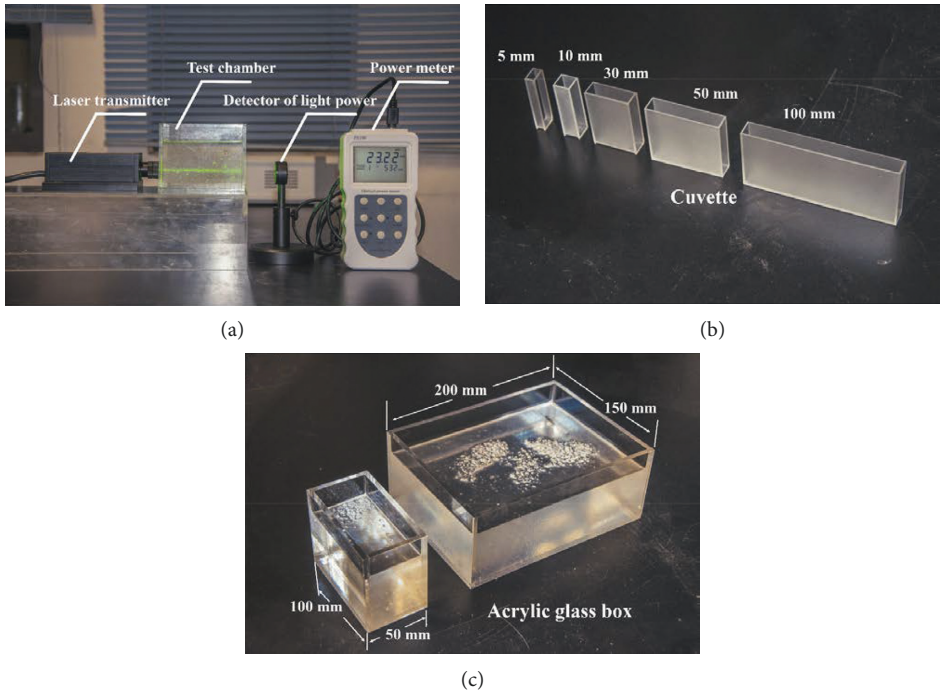

Figure 2: Layout of the experimental apparatus and test chambers.

fused quartz and mineral oil, the experiments are set up to validate that the transmittance of transparent soil is subjected to exponential decay due to viewing depth d and refractive index matching $(n_s - n_l)$.

2.3.2. Impact of Viewing Depth. Assuming that viewing depth d is the single variable in (5), expression of transmittance T is simplified as

$$T = e^{-Kd}, \tag{6}$$

where K refers to the attenuation coefficient. In practice, (6) is also deduced from the Beer–Lambert law [27]. According to the Beer–Lambert law, the light that is absorbed by a substance is proportional to its transmitted thickness. In particular, transmitted thickness is identified as the viewing depth in this research. Figure 3 reveals the relationship between transmittance T and viewing depth d. For investigated transparent soil with fused quartz, the attenuation coefficient K is calculated to be 0.0021 mm^{-1} based on verification of experimental data. However, deviation ranges exist in the transmittance results, and the confidence interval of mean transmittance is denoted as the error bar in Figure 3.

2.3.3. Impact of Refractive Index Matching. A refractive index matching technique has been applied in various fields of study, including granular media and riverbeds [28]. Further research has also sought to establish a methodology of assessment for allowable refractive index mismatch [22]. In this analysis, to investigate the impact of refractive index matching on transmittance, the matching liquid is prepared with various oil mix ratios to achieve different levels of

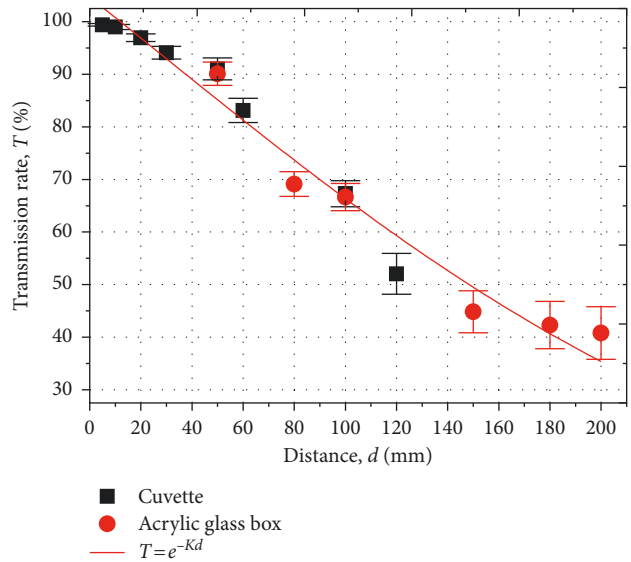

Figure 3: Relationship of transmittance T to viewing depth d.

refractive index matching $(n_s - n_l)$. However, considering that a refractive index of fused quartz n_s remains consistent at room temperature of 20°C, changes in the resulting refractive index of matching liquid n_l represent refractive index matching. Assuming that the refractive index of matching liquid n_l is the single variable in (5), expression of transmittance T is simplified as

$$T = e^{K_1 n_l^2 + K_2 n_l + K_3}, \tag{7}$$

where K_1, K_2, and K_3 refer to the coefficients that are determined by the fitted curve. In Figure 4, the curve fitting

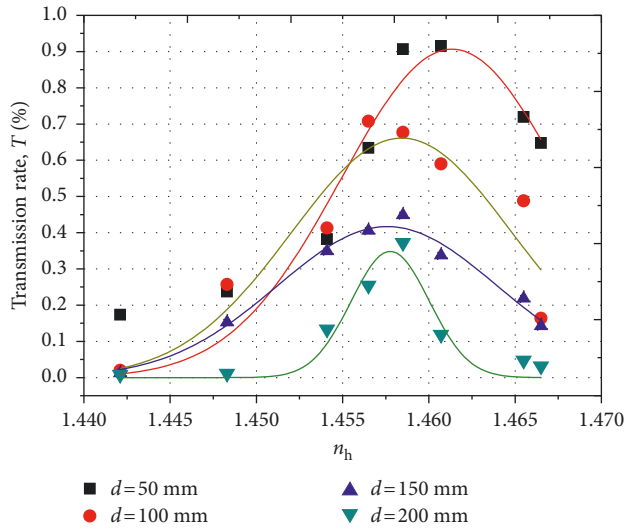

FIGURE 4: Relationship of transmittance T to refractive index matching.

results demonstrate that the transmittance reaches a peak value with the best match of the refractive index matching, whereas there are dips of transmittance as a result of the refractive index mismatch. In general, the impact of refractive index matching is well described by the exponential decay of principle of the Christiansen effect.

3. Relationship between Transmittance and Imaging Quality

3.1. Evaluation Function of Image Clarity. Transmittance describes transparency mathematically, and it is the fidelity in optical measurement of transparent soil that quantification of transparency counts for. Thus, it is necessary to establish the relationship between transmittance and evaluation function of image clarity. For digital image processing of transparent soil, image clarity is the primary concern of DIC precision [29] because captured images within transparent soil consist of different intensities at different pixel positions, which allow for identification. Improved image clarity of image texture is associated with a greater degree of variation in pixel intensity. For example, image intensity changes with the degree of saturation of transparent soil [30–32], with unsaturated transparent soil yielding degraded optical clarity.

Accordingly, the variation in pixel intensity is estimated by the intensity gradient in this research. The intensity gradient is calculated by the Sobel operator, which is prevalently adopted in the image processing technique of edge detection. It calculates the norm of the vector at each pixel of the digital image. By computing the approximated norm of the image gradient at the pixel position (x, y) in the horizontal and vertical directions, the Sobel operator is usually less computationally expensive with an isotropic 3×3 kernel. However, approximations of the derivatives can be defined at higher or lower degrees of accuracy by different kernels. In this paper, the experimental data demonstrate that the approximated results of the isotropic 3×3 gradient Sobel operator are sufficient for distinguishing between different levels of the evaluation function, which corresponds to fidelity in the optical measurements.

As a gradient-based sharpness function in digital photography, the evaluation function E of image clarity of transparent soil is adapted from the Sobel operator. A digital image with $W \times H$ pixels is shown in Figure 5, and the pixel position (x, y) is determined in the following calculations.

Initially, the image intensity of pixel position (x, y) is denoted as $f(x, y)$. $A(x, y)$ is the 3×3 matrix that describes image intensity around pixel position (x, y) in a 3×3 pixel region. Then, 3×3 kernels are utilized in the Sobel operator to convolve with the image intensity $A(x, y)$. As a result, the image gradient vectors at pixel position (x, y) in the horizontal and vertical directions are acquired as $G_x(x, y)$ and $G_y(x, y)$ in (8) and (9), resp.:

$$G_x(x, y) = \begin{bmatrix} -1 & 0 & 1 \\ -2 & 0 & 2 \\ -1 & 0 & 1 \end{bmatrix} * A(x, y), \tag{8}$$

$$G_y(x, y) = \begin{bmatrix} -1 & -2 & -1 \\ 0 & 0 & 0 \\ 1 & 2 & 1 \end{bmatrix} * A(x, y), \tag{9}$$

where $*$ represents a 2-dimensional signal that computes convolution. In other words, $\nabla f(x, y)$ is calculated as

$$\nabla f(x, y) = \left(G_x(x, y), G_y(x, y)\right). \tag{10}$$

Meanwhile, $|\nabla f(x, y)|$ refers to an approximated modulus of the image gradient vector at pixel position (x, y) in a 3×3 pixel region. Thus, $|\nabla f(x, y)|$ is calculated by an image intensity vector from a convolution of the Sobel operator in both the horizontal and vertical directions as follows:

$$|\nabla f(x, y)| = \sqrt{G_x(x, y)^2 + G_y(x, y)^2}, \tag{11}$$

where $G_x(x, y)$ and $G_y(x, y)$ refer to the result of the discrete differentiation operator at pixel position (x, y) in the horizontal and vertical directions, respectively.

The approximated modulus of the image gradient $|\nabla A(x, y)|$ lays the foundation of evaluation function E. Evaluation function E is designated to establish different levels of image clarity. Considering that the mean intensity gradient is proposed to evaluate speckle pattern quality in DIC [33], the evaluation function E is defined as the mean square of the norm of the image gradient at all pixels in the captured image, denoted as follows:

$$E = \sum_{x=1}^{W} \sum_{y=1}^{H} \frac{|\nabla f(x, y)|^2}{N}, \tag{12}$$

where N refers to the sum of pixels in the digital image. In addition, it is noted that the evaluation function given in (12) is sensitive to changes of intensity. Consequently, for comparison between different levels of image clarity, the

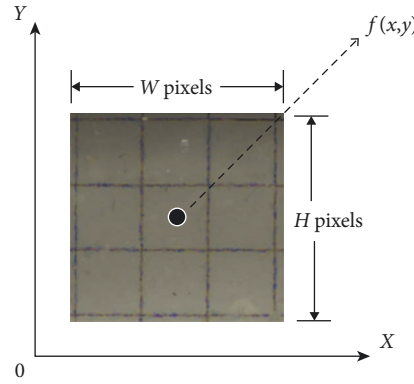

Figure 5: A digital image with $W \times H$ pixels ($x \in [1, W]$; $y \in [1, H]$).

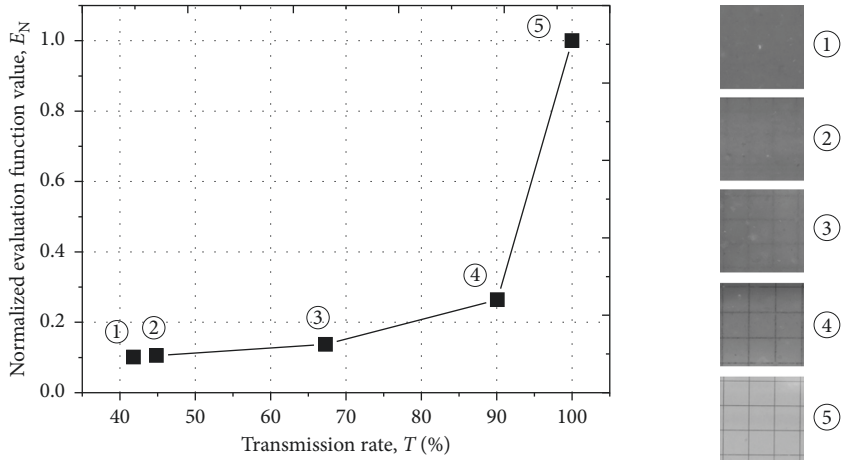

Figure 6: Relevance of transmittance T to the normalized evaluation function of image clarity E_N.

evaluation function E is normalized as E_N in unit-based normalization, expressed as follows:

$$E_N = \frac{E}{E_{max}}, \tag{13}$$

where E_N refers to the normalized evaluation function and E_{max} is determined by the evaluation function of image clarity with no degradation in transparent soil. Image clarity of transparent soil is quantitatively evaluated using the normalized evaluation function E_N.

3.2. Relevance of Transmittance to the Normalized Evaluation Function for Transparent Soil with Fused Quartz. As shown in Figure 6, the relevance of transmittance to image clarity is revealed by the relationship between transmittance T and the normalized evaluation function E_N. Such relevance is investigated for transparent soil with fused quartz. In detail, grid lines are uniformly printed on paper but are viewed through transparent soil with varied depth. Different sizes of the acrylic glass box are utilized for the test chamber containing the transparent soil to determine the viewing depth. For various viewing depths, images of grid lines are captured by a Nikon D7000 digital camera with a 50 mm f/1.8 D lens. Such photographic equipment produces images with a resolution of 4928×3264 pixels by an aperture of f/22, an exposure time of 5 s, and ISO100. For digital image processing, the digital images are cut to the same size for calculation of the evaluation function E_N that defines the image clarity. To capture digital images ①~⑤ in Figure 6, configuration of the photographic equipment and alignment of the optical system are made consistent in each measurement, while transmittance of the transparent soil sample varies from case to case. Meanwhile, transmittance T of transparent soil is measured in each case. As a result, the correlation of transmittance to image clarity is revealed by the relevance of transmittance T to the evaluation function of E_N in Figure 6. Figure 6 includes representative results of transmittance for varied image clarity of transparent soil at the viewing depths of 50 mm (⑤), 100 mm (④), 150 mm (③), and 200 mm (②). In addition, when no transparent soil is in the test chamber, digital image ① is captured and the transmittance of the test chamber without transparent soil is detected.

For transparent soil with fused quartz and mineral oil, the experimental data show a significant increase in image clarity with transmittance higher than 90% (digital image ② with a transmittance of 90.09 ± 2.22%). In addition, based on previous research of portraying the level of transparency [15], the viewing depth of transparent soil in the test was

typically 50 mm. Thus, the digital image ③ delivers a transmittance of 67.29 ± 2.59%, which corresponds to a viewing depth of 50 mm. To draw a conclusion, for some categories of transparent soil such as the soil sample with fused quartz, there is a certain calibration curve as shown in Figure 6 that indicates the relationship between transmittance and imaging quality. And such relationship shall be of great value in further research into accuracy of digital image analysis.

4. Conclusions

The fundamental purpose of this paper is to propose an objective framework for quantification of transparency in transparent soil based on transmittance. In this framework, experimental apparatuses including laser transmitter and power meter are introduced in the measurement method for transmittance. Additionally, analysis of transparent soil property and the principle of the Christiansen effect are integrated in this paper. The principle of the Christiansen effect is proposed to govern the variation in transmittance and to investigate the impact factors that affect transmittance. Furthermore, the relationship between transmittance and imaging quality is also investigated.

On a basis of experimental results, exponential decay of transmittance is validated, and the dominant factors that affect variation in transmittance are viewing depth and refractive index matching. Besides, according to the relevance of transmittance to the evaluation function of the intensity variation, imaging quality of geotechnical modeling with transparent soil is enhanced with increasing transmittance, and imaging quality shows a remarkable improvement when transmittance is greater than 90%.

Above all, the principle of the Christiansen effect provides guidance for increasing the viewing depth of transparent soil and refining the refractive index matching technique to improve transparency in transparent soil in geotechnical modeling. Meanwhile, the relationship between transmittance and image clarity is established. Such relationship lays a foundation of further research regarding the accuracy of digital image analysis in transparent soil with different transmittance.

Conflicts of Interest

The authors declare that they have no conflicts of interest.

Acknowledgments

This work was supported by the National Natural Science Foundation of China (no. 51579219).

References

[1] M. Iskander, *Modeling with Transparent Soils, Visualizing Soil Structure Interaction and Multi Phase Flow, Non-Intrusively*, Springer, New York, NY, USA, 2010.

[2] P. Kelly, *Soil structure interaction and group mechanics of vibrated stone column foundations*, Ph.D. Thesis, University of Sheffield, Sheffield, UK, 2013.

[3] R. Mannheimer, *Slurries You Can See Through, Technology Today*, Southwest Research Institute, San Antonio, TX, USA, 1990.

[4] M. Iskander, J. Lai, C. Oswald, and R. Mannheimer, "Development of a transparent material to model the geotechnical properties of soil," *Geotechnical Testing Journal*, vol. 17, no. 4, pp. 425–433, 1994.

[5] R. J. Mannheimer and C. J. Oswald, "Development of transparent porous media with permeabilities of soils and reservoir materials," *Ground Water*, vol. 31, no. 5, pp. 781–788, 1993.

[6] M. Iskander, S. Sadek, and J. Liu, "Optical measurement of deformation using transparent silica gel to model sand," *International Journal of Physical Modelling in Geotechnics*, vol. 2, no. 4, pp. 13–26, 2003.

[7] K. Tabe, "Transparent aquabeads to model LNAPL Ganglia migration through surfactant flushing," *Geotechnical Testing Journal*, vol. 38, no. 5, pp. 787–804, 2015.

[8] F. M. Ezzein and R. J. Bathurst, "A transparent sand for geotechnical laboratory modeling," *Geotechnical Testing Journal*, vol. 34, no. 6, pp. 590–601, 2011.

[9] J. Wallace and C. Rutherford, "Geotechnical properties of Laponite RD," *Geotechnical Testing Journal*, vol. 38, no. 5, pp. 574–587, 2015.

[10] Z. Song, Y. Hu, C. O'Loughlin, and M. F. Randolph, "Loss in anchor embedment during plate anchor keying in clay," *Journal of Geotechnical & Geoenvironmental Engineering*, vol. 135, no. 10, pp. 1475–1485, 2009.

[11] E. Suescun-Florez, M. Iskander, V. Kapila, and R. Cain, "Geotechnical engineering in US elementary schools," *European Journal of Engineering Education*, vol. 38, no. 3, pp. 300–315, 2013.

[12] S. Kashuk, R. Mercurio, and M. Iskander, "Visualization of dyed NAPL concentration in transparent porous media using color space components," *Journal of Contaminant Hydrology*, vol. 162, pp. 1–16, 2014.

[13] M. Iskander, R. Bathurst, and M. Omidvar, "Past, present, and future of transparent soils," *Geotechnical Testing Journal*, vol. 38, no. 5, pp. 557–573, 2015.

[14] S. Sadek, M. Iskander, and J. Liu, "Accuracy of digital image correlation for measuring deformations in transparent media," *Journal of Computing in Civil Engineering*, vol. 17, no. 2, pp. 88–96, 2003.

[15] J. Liu and M. G. Iskander, "Modelling capacity of transparent Soil," *Canadian Geotechnical Journal*, vol. 47, no. 4, pp. 451–460, 2010.

[16] S. A. Stanier, *Modelling the behaviour of helical screw piles*, Ph. D. Thesis, University of Sheffield, Sheffield, UK, 2011.

[17] J. A. Black and W. A. Take, "Quantification of optical clarity of transparent soil using the modulation transfer function," *Geotechnical Testing Journal*, vol. 38, no. 5, pp. 588–602, 2015.

[18] J. M. Palmer and B. G. Grant, *The Art of Radiometry*, SPIE Press, Bellingham, WA, USA, 2010.

[19] I. H. Malitson, "Interspecimen comparison of the refractive index of fused silica," *Journal of the Optical Society of America*, vol. 55, pp. 1205–1208, 1965.

[20] I. Guzman, M. Iskander, E. Suescun, and M. Omidvar, "A transparent aqueous-saturated sand-surrogate for use in physical modeling," *Acta Geotechnica*, vol. 9, no. 2, pp. 187–206, 2014.

[21] Y. P. Zhang, L. Li, and S. Z. Wang, "Experimental study on pore fluid for forming transparent soil," *Journal of Zhejiang University (Engineering Science)*, vol. 48, no. 10, pp. 1828–1834, 2014.

[22] J. A. Dijksman, F. Rietz, K. A. Lorincz, M. Van Hecke, and W. Losert, "Refractive index matched scanning of dense granular materials," *Review of Scientific Instrument*, vol. 83, article 011301, 2012.
[23] J. W. Gooch, *Encyclopedic Dictionary of Polymers*, Springer, New York, NY, USA, 2011.
[24] C. V. Raman and K. S. Viswanathan, "A generalised theory of the Christiansen experiment," *Proceedings of the Indian Academy of Science*, vol. 41, no. 2, pp. 55–60, 1955.
[25] S. Kang, D. E. Day, and J. O. Stoffer, "Measurement of the refractive index of glass fibers by the Christiansen-Shelyubskii method," *Journal of Non-Crystalline Solids*, vol. 220, no. 2, pp. 299–308, 1997.
[26] A. K. Varshneya, M. C. Loo, and T. F. Soules, "Glass inhomogeneity measurement using the Shelyubskii method," *Journal of the American Ceramic Society*, vol. 68, no. 7, pp. 380–385, 2010.
[27] A. Sassaroli and S. Fantini, "Comment on the modified Beer-Lambert law for scattering media," *Physics in Medicine and Biology*, vol. 49, no. 14, pp. 255–257, 2004.
[28] A. E. Lobkovsky, A. V. Orpe, R. Molloy, A. Kudrolli, and D. H. Rothman, "Erosion of a granular bed driven by laminar fluid flow," *Journal of Fluid Mechanics*, vol. 605, pp. 47–58, 2008.
[29] W. A. Take, "Thirty-Sixth Canadian Geotechnical Colloquium: advances in visualization of geotechnical processes through digital image correlation," *Canadian Geotechnical Journal*, vol. 52, no. 9, pp. 1199–1220, 2015.
[30] S. B. Peters, G. A. Siemens, W. A. Take, and F. Ezzein, "A transparent medium to provide a visual interpretation of saturated/unsaturated hydraulic behavior," in *Proceedings of GeoHalifax*, pp. 59–66, Halifax, Nova Scotia, Canada, 2009.
[31] G. A. Siemens, S. B. Peters, and W. A. Take, "Comparison of confined and unconfined infiltration in transparent porous media," *Water Resources Research*, vol. 49, no. 2, pp. 851–863, 2013.
[32] G. A. Siemens, W. A. Take, and S. B. Peters, "Physical and numerical modeling of infiltration including consideration of the pore air phase," *Canadian Geotechnical Journal*, vol. 51, no. 12, pp. 1475–1487, 2014.
[33] B. Pan, Z. Lu, and H. Xie, "Mean intensity gradient: an effective global parameter for quality assessment of the speckle patterns used in digital image correlation," *Optics & Lasers in Engineering*, vol. 48, no. 4, pp. 469–477, 2010.